JOURNAL OF GUIDANCE, CONTROL, AND DYNAMICS
Vol. 19, No. 1, January–February 1996

Atmospheric Re-Entry Control for Low Lift/Drag Vehicles

Alberto Cavallo*
Seconda Università di Napoli, 81031 Aversa, Italy
and
Ferdinando Ferrara†
Centro Italiano Ricerche Aerospaziali, S.p.A., 81043 Capua, Italy

The re-entry trajectory control of a low lift/drag (L/D) (L/D < 1 sphere-cone shapes) re-entry vehicle is dealt with. The proposed control strategy is based on the linear quadratic regulator (LQR) design technique and on the variable structure systems (VSS) mathematical machinery. The LQR results from the solution of a differential Riccati equation based on the linearization of the equations of motion along a nominal re-entry trajectory. Its objective is the control of the vehicle in the altitude–velocity plane (vertical plane). Terminal control is performed taking into account the range to go in the LQR and by pointing the velocity vector towards the target via a VSS strategy. A single control variable is considered, namely the bank angle, while the angle of attack is kept constant to assure the required L/D. The proposed technique is applied to the assured crew return vehicle re-entry mission in presence of off-nominal aerodynamic and atmospheric and initial conditions. Extreme cases results and a Monte Carlo simulation are presented to test the robustness of the proposed control strategy, which show that the target point is reached with an accuracy of 1 km in more than 50% of the cases and the required 7.6-km maximum error is not exceeded with probability larger than 0.9.

Nomenclature

A_{ref} = reference area
$A(t)$ = linearized system dynamical matrix
$b(t)$ = linearized system input vector
C_D = drag coefficient
C_L = lift coefficient
D = drag force
g = acceleration of gravity
g_0 = acceleration of gravity at sea level
L = lift force
m = mass of the vehicle
P_f = terminal state weighting matrix
$P(t)$ = solution of the differential Riccati equation
Q = state weighting matrix
R = input weight
$\mathcal{R}$ = controllability matrix
R_E = radius of the Earth
R_{TG} = range to go
r = distance from the Earth's center
t = flight time
V = Earth relative speed
X_D = downrange
x = full state vector
x_1 = vertical plane state vector
$\hat{x}_1$ = reference state vector
Y_D = cross range
α = angle of attack
β = sideslip angle
γ = flight-path angle
δx_1 = state error vector
$\delta\sigma$ = bank angle error
θ = geocentric longitude
μ = Earth's gravitational constant
ρ = atmospheric density
σ = bank angle
$\hat{\sigma}$ = reference bank angle
ϕ = geocentric latitude
ψ = heading angle
ω = Earth's angular velocity

Received June 14, 1994; revision received Feb. 24, 1995; accepted for publication June 26, 1995.

*Researcher, Dipartimento di Ingegneria, Real Casa dell'Annunziata, Via Roma 29.
†Control Engineer, Flight Mechanics and Control Department, Via Maiorise.

Introduction

A GREAT deal of current research in space activities is oriented towards design and development of space stations and orbiting laboratories to allow permanent manned presence in space. In such a project the problem of low-cost transportation becomes crucial. Normal operation, like crew rotation and resupply, can be supported with a Space Shuttle Orbiter. However, it is impractical to keep a Shuttle always in readiness to face any possible event, such as an emergency requiring an immediate evacuation of all or part of the crew. Economic alternatives to the Space Shuttle are reusable payload vehicles with low lift-to-drag (L/D) ratio, like the assured crew return vehicle (ACRV) that could be docked to the space station and available for immediate undocking, deorbit, and return to Earth. Its feasibility has been investigated in the United States[1] and in Europe,[2] and its main objectives have been identified as 1) providing emergency return of a seriously ill or injured crew member, 2) providing immediate crew return when an emergency requires evacuation of the station, and 3) providing crew return from the station if the Space Shuttle is not available in the time frame needed. Thus, the vehicle is fundamentally a re-entry vehicle capable of returning the crew to Earth and landing safely and accurately in spite of the vehicle's limited aerodynamics to avoid an expensive recovery and long turnaround periods.

The typical ACRV mission can be composed of three phases: 1) the retreat, in which the vehicle is ejected by the space station and reaches the parking orbit; 2) the orbital flight, in which the deorbit boost is performed to reduce the vehicle velocity and the perigee altitude to obtain the required flight-path angle and the desired velocity at the edge of the atmosphere; then the vehicle covers an orbital arc until it reaches the atmosphere re-entry point, usually located at 120 km altitude; and 3) the atmospheric flight composed of a) re-entry: the ACRV shall stay in the re-entry corridor with upper bounds defined by maximum C_L and lower bounds by upper limits on the load factor, pressure, and heat flux; b) parachute flight: the drogues are opened at a prescribed altitude to stabilize the vehicle and to reduce its velocity, then parachutes are opened; and c) landing: retrorockets are used to reduce the deceleration at impact.

In this paper we address the control of a low L/D vehicle (i.e., Apollo-like shaped vehicles, with L/D value of 0.3) during the

re-entry phase. Traditionally, two control strategies are used in the re-entry phase[3]: 1) guidance using predicted capability, in which the controller computes the path to reach the desired destination starting from the measured actual state variables and 2) guidance using a precomputed nominal path stored on board, in which the objective of the controller is to contrast the variations of the measured state variables from the stored values. In both cases heating and acceleration limits must be taken into account; in the first strategy this generates a set of constraints in the actual path definition, whereas in the second one the limits are considered during the phase of nominal trajectory computation. Moreover, the control system must provide a certain degree of robustness against off-nominal entry conditions, aerodynamic uncertainties, and atmospherical disturbances.

Prediction methods are based on the computation of future trajectories. The main drawback of this technique is the high computational burden, which does not seem appropriate for small payload vehicles. Several techniques have been proposed to overcome this problem, among which are numerical fast-time algorithms (collocation methods[4,5]) or approximate closed-form (see Ref. 6 and references therein) solutions of the equations of motion, eventually combined with optimization procedures to satisfy performance requirements, or, recently, the use of neural networks.[7]

Nominal trajectory methods are based on the classic concepts of tracking and regulation systems. Namely, the tracking error, i.e., the difference between desired and actual trajectory, is input to a controller that acts to reduce the error and steer the vehicle onto the nominal trajectory. Since the design of the controller is more easily done in the linear time-invariant setting, the commonly used approach is to consider a single equilibrium point and obtain a linear time-invariant model of the plant to be controlled. Unfortunately this is not the case for a vehicle in the re-entry phase. Indeed, the model can still be linearized, but along a reference trajectory, not at a single point. The result of such a process is a linear time-varying system. Linear time-varying models are considerably harder to treat than invariant ones, both for the analysis of structural properties, such as controllability and stability, and for the reduced availability of control techniques. The nominal trajectory guidance method stores the state variables and the feedback control gains, as a function of a given independent variable along the path. The independent variable may be the obvious quantity time, or it may consist of one state variable or some combinations of several of them. In the Shuttle, for example, a drag vs velocity schedule is stored in the onboard computer. The drag profile is corrected in flight to follow a prescribed path and, based on ranging techniques,[8] to reach the desired target point. Final cross-range errors are corrected performing bank maneuvers. Further researches investigate whether path following guidance is effective in controlling the re-entry trajectory of a low L/D vehicle[9,10] in the presence of perturbations.

In this paper, we approach this problem using linear quadratic (LQ) and variable structure systems (VSS) techniques. More specifically, an LQ time-varying controller is designed to follow a prescribed trajectory in the vertical plane and recover final displacement errors, whereas a VSS strategy is used to point the vehicle velocity vector towards the target. From a practical point of view the proposed strategy is easily implemented on low-cost, low-weight re-entry vehicles because it requires only storing on board a precomputed set of LQ control gains, a reference trajectory, and a navigation system to determine the actual state variables. Finally, the proposed control law has been applied to the ACRV re-entry mission.

Model

To develop our trajectory control problem we have chosen a proposed European vehicle model for the ACRV mission. The equations of motion of an unpowered re-entry vehicle considered as a point mass m flying inside the atmosphere of the spherical rotating Earth are,[11] for the kinematics,

$$\dot{r} = V \sin\gamma \tag{1}$$

$$\dot{\theta} = \frac{V \cos\gamma \cos\psi}{r \cos\phi} \tag{2}$$

$$\dot{\phi} = \frac{V \cos\gamma \sin\psi}{r} \tag{3}$$

and for the dynamics,

$$\dot{V} = -(1/m)D - g\sin\gamma + \omega^2 r \cos\phi(\sin\gamma\cos\phi - \cos\gamma\sin\phi\sin\psi) \tag{4}$$

$$\dot{\gamma} = (1/mV)L\cos\sigma - (g/V)\cos\gamma + (V/r)\cos\gamma + 2\omega\cos\phi\cos\psi + (\omega^2 r/V)\cos\phi(\cos\gamma\cos\phi + \sin\gamma\sin\phi\sin\psi) \tag{5}$$

$$\dot{\psi} = \frac{1}{mV}\frac{L\sin\sigma}{\cos\gamma} - \frac{V}{r}\cos\gamma\cos\psi\tan\phi + 2\omega(\tan\gamma\cos\phi\sin\psi - \sin\phi) - \frac{\omega^2 r}{V\cos\gamma}\sin\phi\cos\phi\cos\psi \tag{6}$$

The state vector of the model is given by the standard Earth-fixed variables

$$x = [r \quad \theta \quad \phi \quad V \quad \gamma \quad \psi]^T \tag{7}$$

and D and L represent the aerodynamic forces acting on the vehicle whose expression is given by

$$L = \tfrac{1}{2}\rho V^2 C_L A_{\text{ref}} \tag{8}$$

$$D = \tfrac{1}{2}\rho V^2 C_D A_{\text{ref}} \tag{9}$$

Data to model the density of the Earth's atmosphere are taken from the U.S. Standard Atmosphere 1976; winds are not considered during simulations. For the gravity forces, a Newtonian gravity law $g = \mu/r^2$ is assumed.

The vehicle has an Apollo-like shape with a maximum diameter of 4.5 m and a height of 4.6 m. The total mass is 6000 kg with six crew members. The L/D ratio necessary to meet the requirement of 100-km cross range has been found to be 0.3. This ratio is obtained with a constant angle of attack of about 20 deg. For illustrative purposes drag and lift coefficients are assumed to remain constant with Mach number values. The vehicle is aerodynamically stabilized via a trim ballast mass and the attitude is controlled by means of reaction jets.

Since the angles of attack and sideslip are assumed to be constant along the trajectory ($\alpha = 20$ deg and $\beta = 0$ deg), the only control variable is the bank angle σ. The mission requirements concern the landing accuracy; in particular they prescribe an accuracy of 7.6 km at 1σ at the drogue opening (7-km altitude). To satisfy such requirements it is convenient to introduce two auxiliary variables, namely downrange and cross range. The cross range of a particular trajectory point is defined as the perpendicular distance from the point to the initial great circle measured on the Earth surface. Downrange is then the distance along the initial great circle from the initial point to the point at which the cross range is measured. The initial great circle is defined by the initial heading at the initial latitude and longitude point $L(\theta_0, \phi_0)$ (see Fig. 1). Then for the point $F(\theta, \phi)$ the downrange X_D and the cross range Y_D are defined by

$$X_D = R_E \cos^{-1}\left\{\frac{\cos LF}{\cos[\sin^{-1}(\sin LF \sin\xi)]}\right\} \tag{10}$$

$$Y_D = R_E \sin^{-1}(\sin LF \sin\xi) \tag{11}$$

and

$$LF = \cos^{-1}[\sin\phi\sin\phi_0 + \cos\phi\cos\phi_0\cos(\theta - \theta_0)] \tag{12}$$

is the angle subtended by the great circle from the initial point to the actual one, where the subscript 0 refers to initial values, and ξ is angle between the initial great circle and the preceding great circle and its expression is

$$\sin\zeta = \frac{\sin(\theta - \theta_0)\cos\phi}{\sin LF} \tag{13}$$

$$\cos\zeta = \frac{\sin\phi - \sin\phi_0\cos LF}{\cos\phi_0\sin LF} \tag{14}$$

$$\xi = \zeta + \psi_0 - \pi/2 \tag{15}$$

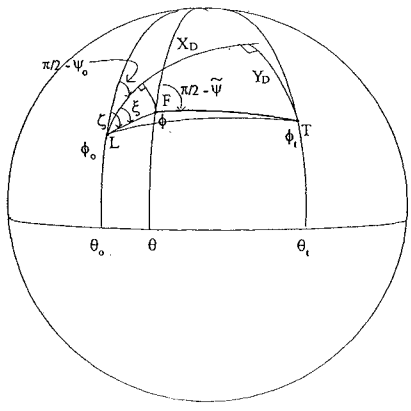

Fig. 1 Downrange, cross-range, and range to go geometry.

Figure 1 shows the downrange and the cross range for the target point $T(\theta_t, \phi_t)$. In the sequel we will consider the range to go as a variable to be controlled, i.e., the distance between the actual position of the vehicle and the target point measured along the great circle through the same points (i.e., arc FT in Fig. 1). It can be expressed as

$$R_{TG} = R_E \cos^{-1}[\sin\phi_t \sin\phi + \cos\phi_t \cos\phi \cos(\theta_t - \theta)] \quad (16)$$

where the subscript t refers to the target point. Its differential equation is

$$\dot{R}_{TG} = -(R_E/r)V \cos\gamma \cos(\tilde{\psi} - \psi) \quad (17)$$

where $\tilde{\psi}$ is given by

$$\tilde{\psi} = \frac{\pi}{2} - \tan^{-1} \frac{\sin(\theta_t - \theta)\cos\phi_t \cos\phi}{\sin\phi_t - \sin\phi \cos(R_{TG}/R_E)} \quad (18)$$

From a computational point of view, the inverse tangent must be computed on four quadrants using Eqs. (13) and (14). Geometrically R_{TG} is a curvilinear abscissa along the preceding great circle, with its origin at the target point, and $\tilde{\psi}$ is the angle between the local parallel and the FT arc.

Problem Formulation

In this section we discuss the control strategy to track the reference trajectory and address some controllability problems arising from this approach. We can approximately decouple the control in the vertical plane (i.e., the r–V–γ plane) from that along its perpendicular direction. Then we can select a control strategy for the vertical plane independently from that needed to control in the orthogonal direction. This statement can be easily proved considering that, if we neglect Coriolis and centrifugal forces, the set of equations describing the motion of the vehicle in the vertical plane, (1), (4), and (5), involve only the variables r, V, and γ. This assumption is valid because the low L/D results in limited cross range and the entry duration is brief. Moreover, since the nominal behavior of the variable R_{TG} depends on the same variables, it can be controlled with the same variables if we require that the vehicle flies straight to the target ($\psi = \tilde{\psi}$). Nevertheless, in the case of off-nominal atmospheric or aerodynamic conditions, even perfect (r, V, γ) tracking would result in a range to go offset; thus an additional R_{TG} feedback should be considered to meet the landing accuracy. Finally, note that the sign of the control variable σ does not affect the preceding equations. Any control strategy in the vertical plane gives a degree of freedom on the sign of the global control variable σ. This degree of freedom will be used to control the error in the orthogonal direction. In particular, according to the considerations of the previous section, the selected control strategy is to define a control law such that the vehicle velocity will point to the target. Hence we define the heading error angle as $\psi - \tilde{\psi}$, i.e., the angle between the actual velocity vector and a vector from the vehicle to the target point.

These remarks lead to the following control strategy:

1) Keep the vehicle around both the nominal trajectory in the vertical plane and the nominal range to go profile.

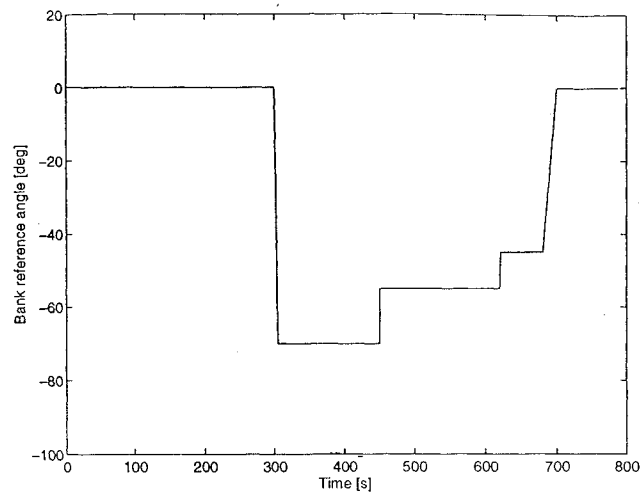

Fig. 2 Nominal bank angle.

2) Point the vehicle towards the target by means of bank reversal maneuvers.

The first objective can be accomplished by using an LQ control strategy. In particular, approximations and errors mentioned earlier, due to modeling errors, changes in the air density, etc., are supposed to be absorbed by the well-known robustness properties of the full-state feedback LQ regulator. To accomplish the second objective the designer has at disposal only the sign of the control variable. This consideration leads to the selection of a VSS control strategy, in which the sliding manifold is defined by the heading error angle.

The nominal trajectory has been obtained by means of an optimization code[12] that minimizes the total thermal load taking into account path constraints on the load factor (i.e., $\sqrt{(L^2 + D^2)}/mg_0$ with prescribed maximum value of 4 g), maximum stagnation point heating rate of 600 kW/m^2, and terminal path constraints (i.e., relative speed between 90 and 110 m/s and flight-path angle between -80 and -60 deg). The nominal bank angle $\hat{\sigma}$ is shown in Fig. 2. Moreover, in computing the nominal trajectory bank reversal maneuvers have been performed to assure a nominal 100-km cross range.

To design the LQ controller we will linearize the equations along the nominal trajectory. We conclude this section with some consideration about the controllability of a linear system. It is well known that in the case of time-varying bounded linear systems (i.e., systems whose matrices are bounded for all t) the uniform complete controllability should be checked by testing the positive definiteness of the controllability gramian $W(t, t + \lambda)$, defined by

$$W(t, t + \lambda) = \int_t^{t+\lambda} \Phi(t, \tau) B(\tau) B^T(\tau) \Phi^T(t, \tau)\, d\tau \quad (19)$$

where $\Phi(t, \tau)$ and $B(t)$ are the transition and input matrices respectively. Obviously this condition is not easy to check; then we recall the definition of instantaneous controllability.[13]

Definition. A linear time-varying system is instantaneously controllable if and only if, at any time t, the state can be made to jump from its current value $x(t^-)$ to an arbitrary value $x(t^+)$, by means of an impulse input function u of order at most $n - 1$, where n is the order of the system. □

The test for instantaneous controllability is considerably simpler than that for uniform complete controllability, involving only the matrix $A(t)$ and the vector $b(t)$, as in the time-invariant case. Indeed, if the matrices $A(t)$ and $B(t)$ are supposed to be continuously differentiable at least $n - 1$ and n times, respectively, it is sufficient to check the condition rank $\mathcal{R} = n$ for all t,

$$\mathcal{R} = \left[B(t)\ L_A B(t)\ \cdots\ L_A^{n-1} B(t)\right] \quad (20)$$

and $L_A B(t)$ is the Lie derivative defined by

$$L_A B(t) = A(t)B(t) - \dot{B}(t) \quad (21)$$

Generally, instantaneous controllability neither implies nor is implied by uniform complete controllability. However, it is possible to show[14] that in the single-input case bounded systems whose controllability matrix is bounded (i.e., its norm is bounded) with its inverse and its derivative are uniformly completely controllable.

To test the preceding condition in the present case a certain degree of smoothness in the bank maneuver must be assumed. This assumption is true from a practical point of view because the propulsive moments used to steer the bank angle do not present cusp. The proposed test shows that the vehicle is not controllable on the nominal trajectory when the bank angle is zero. This can be easily realized from a physical point of view, because when the bank angle is zero the vehicle cannot increase the vertical lift. Thus during the first 300 s and the last 80 s (see Fig. 2) the vehicle cannot be controlled and is left uncontrolled.

Control

In this section we describe in detail the control strategy used to reach the parachute deployment area. As mentioned earlier, the first step is to design an LQ control to meet the nominal altitude, relative speed, and flight-path angle. The range to go R_{TG} is also controlled to meet the landing accuracy. The equations describing the dynamic behavior of these variables are Eqs. (1), (4), (5), and (17).

The first step is to linearize these equations along the nominal trajectory; the linearization procedure is standard, i.e., we define a perturbed state $\delta x_1 = [\delta r,\ \delta V,\ \delta\gamma,\ \delta R_{TG}]^T$ such that $x_1 = \hat{x}_1 + \delta x_1$, and analogously a perturbed control variable $\delta\sigma = \sigma - \hat{\sigma}$. Then Eqs. (1), (4), (5), and (17) can be written in linearized form as

$$\delta\dot{x}_1 = A(t)\delta x_1 + b(t)\delta\sigma \tag{22}$$

As mentioned in the previous section, to decouple these equations from the remaining ones, we must neglect the Earth rotation ($\omega = 0$). This approximation can be considered as a modeling error to be rejected by the LQ controller.

The cost functional J we have considered is the classical finite horizon LQ criterion functional[15]

$$J = \delta x_1^T(t_f)P_f\delta x_1(t_f) + \int_0^{t_f}\left[\delta x_1^T(\tau)Q\delta x_1(\tau) + R\delta\sigma^2(\tau)\right]d\tau \tag{23}$$

where $R > 0$, P_f, and Q are positive semidefinite, and t_f is the nominal parachute deployment time. It is well known that the state feedback control policy that minimizes the index J is given by

$$\delta\sigma(t) = -\frac{b^T(t)P(t)\delta x_1(t)}{R} = -K(t)\delta x_1(t) \tag{24}$$

$$-\dot{P} = A^TP + PA - (1/R)Pbb^TP + Q \tag{25}$$

$$P(t_f) = P_f \tag{26}$$

The crucial point in the LQ procedure is the selection of the weighting matrices. Several empirical laws have been proposed to give the designer effective guidelines. According to Ref. 16 we have chosen diagonal weighting matrices with

$$P_{fii} = \frac{1}{\delta\bar{x}_{1,i}^2(t_f)} \tag{27}$$

and

$$Q_{ii} = \frac{1}{t_f\delta\bar{x}_{1,i}^2} \tag{28}$$

$$R = \frac{1}{t_f\delta\bar{\sigma}^2} \tag{29}$$

where the overbar refers to the maximum acceptable value.

With this choice the weighting matrices are

$$P_f = \mathrm{diag}\left[\frac{1}{500^2},\ 1,\ \left(\frac{180}{2\pi}\right)^2,\ \frac{1}{1000^2}\right] \tag{30}$$

$$Q = \frac{1}{400}\mathrm{diag}\left[\frac{1}{5000^2},\ \frac{1}{50^2},\ \left(\frac{180}{5\pi}\right)^2,\ \frac{1}{10000^2}\right] \tag{31}$$

$$R = \frac{1}{400}\left(\frac{180}{20\pi}\right)^2 \tag{32}$$

In Fig. 3 the feedback gains on altitude (rad/m), relative speed (rad · s/m), and downrange (rad/m) errors are shown.

A limiter has been introduced to keep σ in the range [−180 deg, 0 deg]. This is because in the presence of heavy disturbances the controller tries to increase the magnitude of the correcting input signal, and this can cause a lack of accuracy in the linearization. Indeed, from a physical point of view it is obvious that the closer the bank angle is to 0 deg, the higher the vertical lift is, but when the bank angle exceeds this limit, the vertical lift decreases, and this phenomenon is not modeled in the linearized system. Moreover this sign change in the bank angle would act unfavorably also on the heading control.

The control used to assure the desired cross range is obtained via a VSS strategy. In particular, we have defined a sliding manifold s as the heading angle error, i.e.,

$$s = \tilde{\psi} - \psi \tag{33}$$

Then the commanded bank angle is

$$\sigma_C = |\sigma|\mathrm{sign}(s) \tag{34}$$

The existence of the sliding motion is complex to prove in the general case, but under the hypothesis of a flat Earth it can be easily proved. In this case the equations of motions become

$$\dot{X} = V\cos\gamma\cos\psi \tag{35}$$

$$\dot{Y} = V\cos\gamma\sin\psi \tag{36}$$

$$\dot{\psi} = -\frac{L\sin\sigma}{mV\cos\gamma} \tag{37}$$

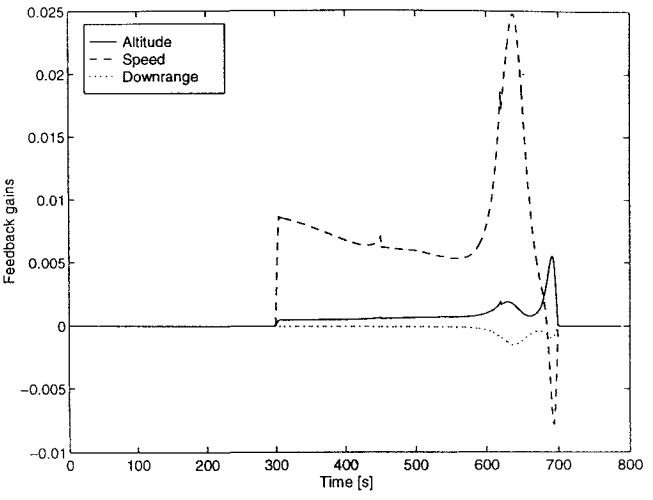

Fig. 3 Feedback gains.

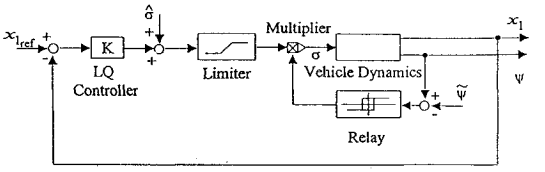

Fig. 4 Global control scheme; $x_1 = [r, V, \gamma, R_{TG}]^T$ is the partial state controlled via LQ.

and then $\tilde{\psi}$ can be written as

$$\tilde{\psi} = \tan^{-1}\left(\frac{Y_t - Y}{X_t - X}\right) \tag{38}$$

where (X, Y) are the coordinates of the actual point in a Cartesian coordinate system with the Z axis directed upwards along the local vertical, and the subscript t refers again to the parachute deployment point. From these equations the condition for the existence of the sliding motion $\dot{s}s < 0$ locally around $s = 0$ (see Ref. 17) can be easily shown to hold.

The bank reversal strategy cannot be implemented as described in Eq. (34), since it would produce commutations at infinite frequency. Moreover, because the vehicle maneuverability is constrained (bounded bank angle rate and acceleration), the bank reversal maneuver will not be instantaneous. To avoid the chattering phenomenon it is well known that in Eq. (34) the signum function can be replaced by a hysteresis loop, whose width is selected according to the maximum admissible heading angle error that we have supposed to be 8 deg in our case.

The overall control scheme is shown in Fig. 4. Note that the reference bank angle entering the LQ controller is computed in the absence of bank reversals since only the VSS strategy is responsible for these maneuvers.

Simulation Results

To evaluate controller performances, several simulations have been performed, and some of these are reported in this section. The effect of off-nominal entry conditions on the relative speed, flight-path angle, and downrange (i.e., initial latitude and longitude) have been considered. Moreover, the lift and drag coefficients have been considered uncertain, together with the model of the atmospheric density. According to Ref. 2 the range of variations for the preceding parameters, derived from an error analysis during the controlled deorbit boost, are shwon in Table 1.

An additional 5% (3σ) constant perturbation on the air density has also been considered. In the sequel we present in detail two simulations.

Case A

In this simulation the parameters are selected according to their values at 1σ in such a way to maximize the L/D ratio, i.e., C_L increased by 10% and C_D decreased by 5%; moreover, the initial speed and the flight-path angle are increased and the downrange error is positive, i.e., the actual entry point is ahead of the nominal one. The results of the simulations are shown in Figs. 5–11 (dashed lines). Indeed, Fig. 5 shows that once the vehicle has reached its nominal altitude, it tries to stay below this reference to recover the range to go error (Fig. 6). Analogously, Fig. 7 shows that the controller tries to slow down the capsule. Figure 9 shows that the load factor history experienced by the controlled vehicle stays close to its nominal value, never exceeding the 4-g limit. The effect of the bank reversals is apparent in Fig. 10, which shows the behavior of the ground track around the target point. Figure 11 depicts the bank angle evolution during re-entry. Roughly speaking, the absolute value of the actual control is larger than its nominal value. This is done to reduce the vertical lift. The roll reversal maneuvers are performed to force the vehicle to point towards the target (see Fig. 10).

Table 1 Parameter nominal values and errors

Perturbed variable	Nominal value	3σ error
v, m/s	7496	±0.62
γ, deg	−1.46	±0.016
X_D, km	0	±80
C_L	0.4	±30%
C_D	1.325	±15%

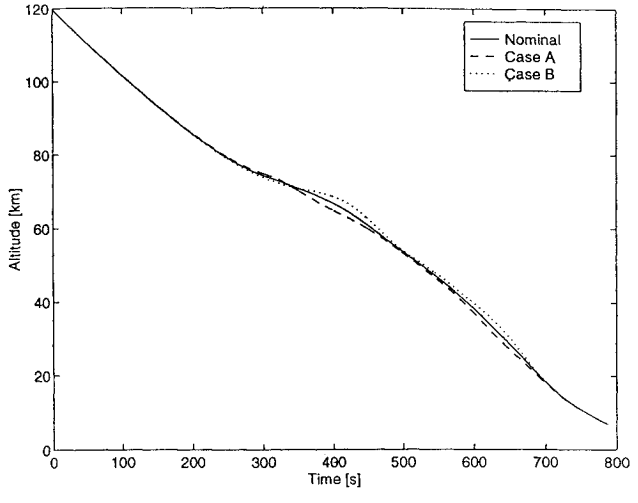

Fig. 5 Altitude–time history.

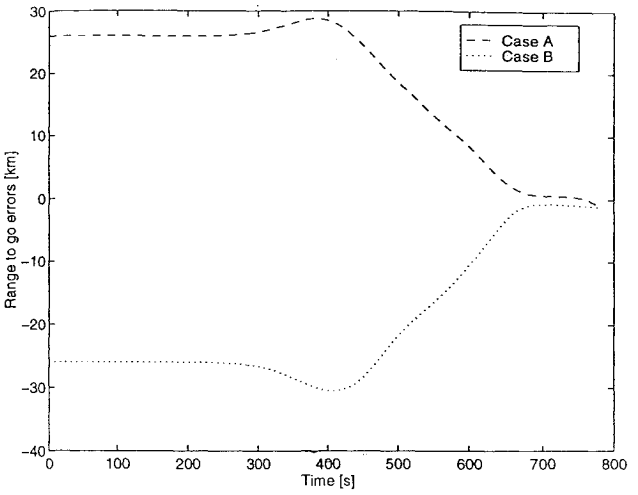

Fig. 6 Range to go error–time history.

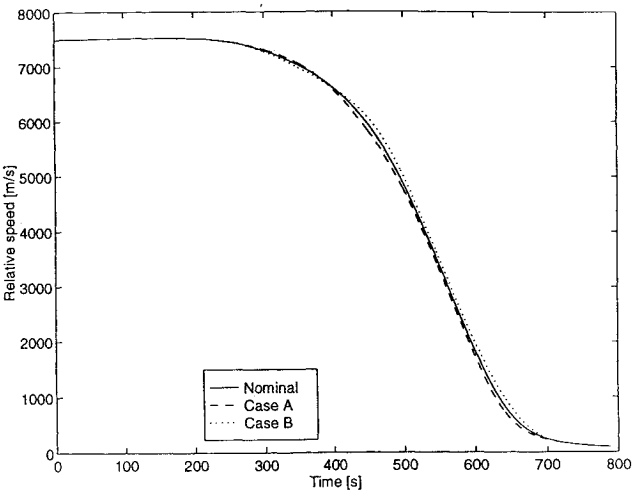

Fig. 7 Earth relative speed–time history.

Case B

This situation is in some sense dual of the preceding one. In fact, the parameter perturbations are selected with opposite sign. The results of the simulations are again shown in Figs. 5–11 (dotted lines). The simulation results are also dual in the same sense. As shown in Fig. 5 the vehicle tries to fly above the nominal altitude to compensate for the L/D reduction. To do this the LQ controller initially sets the bank angle to zero to gain more vertical lift (see Fig. 11). The load factor limit is again not exceeded, as shown in Fig. 9. Figure 10 shows the final portion of the ground track. Note a substantial difference between this case and case A: now the vehicle reaches the target from the opposite side. This is due to the low L/D ratio and consequently to the decreased horizontal lift.

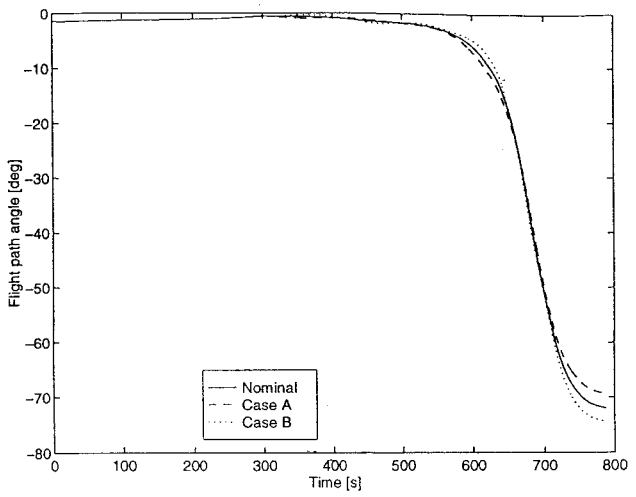

Fig. 8 Flight-path angle–time history.

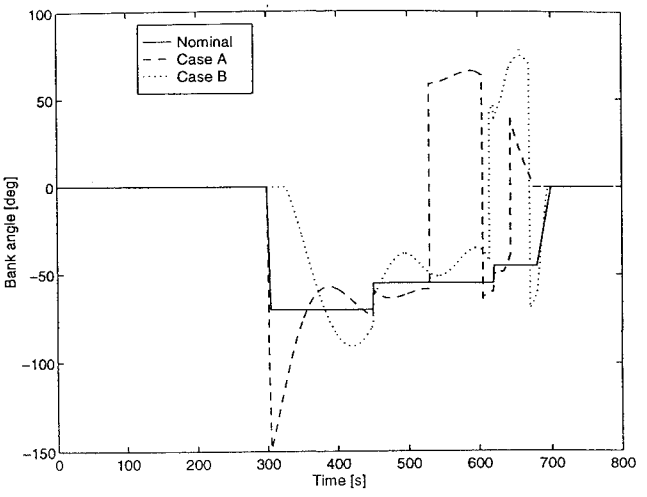

Fig. 11 Bank angle–time history.

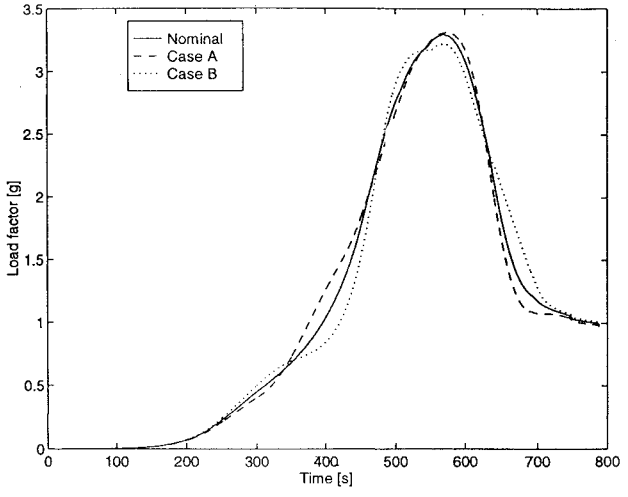

Fig. 9 Load factor–time history.

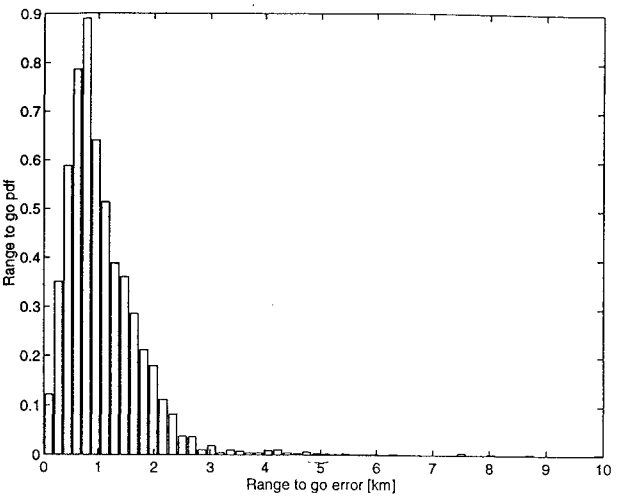

Fig. 12 Range to go error PDF.

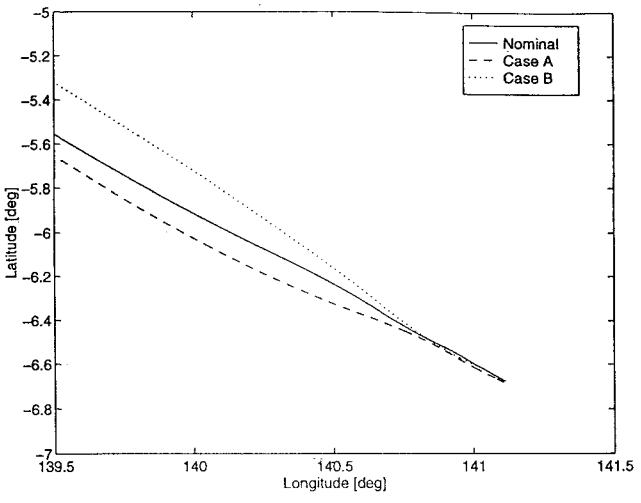

Fig. 10 Ground track.

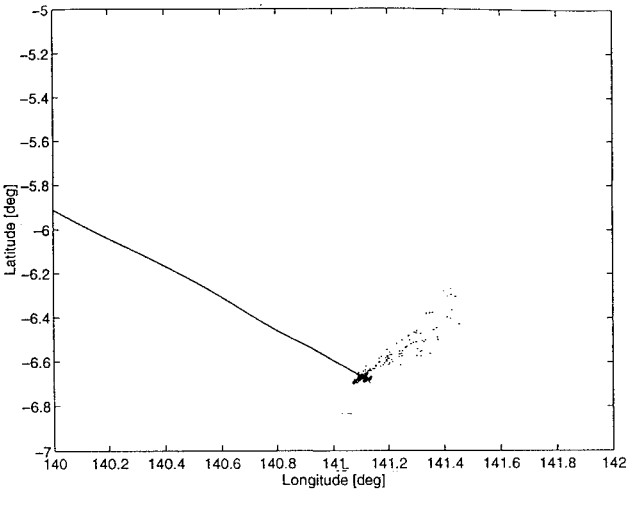

Fig. 13 Target dispersion.

Finally, to test the robustness of the proposed control law, a Monte Carlo simulation has been performed to have a more accurate idea of the dispersions at the target point and the associated probabilities. The statistics of the errors are taken from Table 1. In Fig. 12 a histogram of the probability density function of the range to go error is reported considering 5000 simulations. Note that in more than 50% of the cases the error does not exceed 1 km, and the prescribed 7.6-km error is guaranteed with probability larger than 0.9.

Figure 13 shows the dispersion around the target. The largest errors happen in the case of low horizontal lift due to a bank angle close to zero imposed by the LQ controller to track the trajectory in the vertical plane; then the low horizontal lift causes a larger cross-range error.

Conclusions

In this paper the re-entry trajectory control of a low L/D vehicle has been presented and applied to ACRV. The control strategy is based on LQ and VSS techniques and exhibits strong robustness properties. The equations of motion of the vehicle are linearized along the reference trajectory defined by altitude, relative speed,

flight-path angle, range to go, and a nominal bank guidance law necessary to assure a required cross range of 100 km. Then a time-varying LQ controller can be designed on the linearized model to control the vehicle robustly in the vertical plane. The sign of the bank angle is determined by a VSS controller to point the vehicle velocity vector towards the target. Simulation results are presented, in the case of extreme perturbations of initial conditions, aerodynamic coefficients, and air density, showing the effectiveness of the control strategy. Monte Carlo simulations are also provided to show that the proposed technique fulfills the ACRV mission requirements for the prescribed range of parameter variations.

References

[1]Reding, J. P., and Svendsen, H. O., "Lifting Entry Rescue Vehicle Configuration," *Journal of Spacecraft and Rockets*, Vol. 27, No. 5, 1990, pp. 606–612.

[2]Jallade, S., and Champetier, C., "Assured Crew Return Vehicle GNC Design," Matra Marconi Space, ACRV/RT/SJ/38.92, Toulouse, France, Feb. 1993.

[3]Wingrove, R. C., "A Survey of Atmospheric Re-Entry Guidance and Control Methods," *AIAA Journal*, Vol. 1, No. 9, 1963, pp. 2019–2029.

[4]Hargraves, C. R., and Paris, S. W., "Direct Trajectory Optimization Using Non Linear Programming and Collocation," *Journal of Guidance, Control, and Dynamics*, Vol. 10, No. 4, 1987, pp. 338–342.

[5]Dixon, L. C. W., and Biggs, M. C., "The Advantage of Adjoint Control Transformation when Determining Optimal Trajectories by Pontriagin Maximum Principle," *Journal of the Royal Aeronautical Society*, Vol. 76, March 1972, pp. 169–174.

[6]Wingrove, R. C., "A Study of Guidance to Reference Trajectories for Lifting Re-Entry at Supercircular Velocity," NASA, TR R-151, Dec. 1963.

[7]Ambrosino, G., Ciniglio, U., Ferrara, F., Filippone, E., and Verde, L., "Una Tecnica di Guida Adattativa per il Rientro Aeroassistito di Veicoli Spaziali" (in Italian), *Proceedings of the XII Congresso Nazionale AIDAA* (Como, Italy), 1993, pp. 1519–1529.

[8]Serrano-Martinez, J. B., Baeza-Martin, M., and Delgado-Montes, I., "Study on Aerocapture Guidance and Navigation," Grupo de Mecanica del Vuelo (GMV), S.A., GMVSA 2049/89, Madrid, Spain, March 1989.

[9]Roenneke, A. J., and Cornwell, P. J., "Trajectory Control for Low Lift Reentry Vehicle," *Journal of Guidance, Control, and Dynamics*, Vol. 16, No. 5, 1993, pp. 927–933.

[10]Sworder, D. D., and Wells, G. R., "Guidance Laws for Aerodynamically Controlled Reentry Vehicles," *Journal of Spacecraft and Rockets*, Vol. 14, No. 2, 1977, pp. 111–117.

[11]Vinh, N. X., *Optimal Trajectories in Atmospheric Flight*, Elsevier, New York, 1981.

[12]Capuano, A., Ferrara, F., Marzano, A., and Borriello, G., "Strategie di ottimizzazione di traiettorie e di guida per veicoli di rientro" (in Italian), *Proceedings of the XII Congresso Nazionale AIDAA* (Como, Italy), 1993, pp. 1507–1518.

[13]Silverman, L. M., and Meadows, H. E., "Controllability and Observability in Time-Variable Linear Systems," *SIAM Journal on Control and Optimization*, Vol. 5, No. 1, 1967, pp. 64–73.

[14]Silverman, L. M., and Anderson, B. D. O., "Controllability, Observability and Stability of Linear Systems," *SIAM Journal on Control and Optimization*, Vol. 6, No. 2, 1968, pp. 121–130.

[15]Anderson, B. D. O., and Moore, J. B., *Optimal Control*, Prentice–Hall, New York, 1990.

[16]Bryson, A. E., and Ho, Y. C., *Applied Optimal Control*, Hemisphere, New York, 1975.

[17]Utkin, V. I., *Sliding Modes in Control and Optimization*, Springer–Verlag, Berlin, 1991.